

Mercury Stable Isotopes Reveal Influence of Foraging Depth on Mercury Concentrations and Growth in Pacific Bluefin Tuna

Daniel J. Madigan,^{*,†,∞,¶,||} Miling Li,^{†,∞,||} Runsheng Yin,^{‡,§} Hannes Baumann,^{||} Owyn E. Snodgrass,[⊥] Heidi Dewar,[#] David P. Krabbenhoft,^{§,||} Zofia Baumann,^{||} Nicholas S. Fisher,[∇] Prentiss Balcom,[†] and Elsie M. Sunderland^{†,◆,||}

[†]Harvard John A. Paulson School of Engineering and Applied Science, Harvard University, Cambridge, Massachusetts 02138, United States

[‡]State Key Laboratory of Ore Deposit Geochemistry, Institute of Geochemistry, Chinese Academy of Sciences, Guiyang 550002, China

[§]U.S. Geological Survey, Middleton, Wisconsin 53562, United States

^{||}Department of Marine Sciences, University of Connecticut, Groton, Connecticut 06269, United States

[⊥]Ocean Associates, Southwest Fisheries Science Center, NMFS, NOAA, La Jolla, California 92037, United States

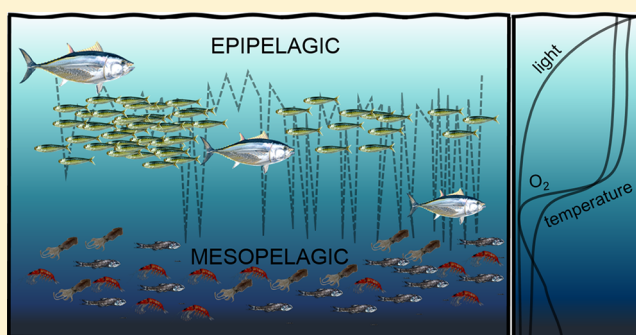
[#]Fisheries Resources Division, Southwest Fisheries Science Center, National Marine Fisheries Service (NMFS), National Oceanic and Atmospheric Administration (NOAA), La Jolla, California 92037, United States

[∇]School of Marine and Atmospheric Sciences, Stony Brook University, Stony Brook, New York 11794, United States

[◆]Department of Environmental Health, Harvard T. H. Chan School of Public Health, Harvard University, Boston, Massachusetts 02138, United States

Supporting Information

ABSTRACT: Pelagic ecosystems are changing due to environmental and anthropogenic forces, with uncertain consequences for the ocean's top predators. Epipelagic and mesopelagic prey resources differ in quality and quantity, but their relative contribution to predator diets has been difficult to track. We measured mercury (Hg) stable isotopes in young (<2 years old) Pacific bluefin tuna (PBFT) and their prey species to explore the influence of foraging depth on growth and methylmercury (MeHg) exposure. PBFT total Hg (THg) in muscle ranged from 0.61 to 1.93 $\mu\text{g g}^{-1}$ dw (1.31 $\mu\text{g g}^{-1}$ dw ± 0.37 SD; 99% $\pm 6\%$ MeHg) and prey ranged from 0.01 to 1.76 $\mu\text{g g}^{-1}$ dw (0.13 $\mu\text{g g}^{-1}$ dw ± 0.19 SD; 85% $\pm 18\%$ MeHg). A systematic decrease in prey $\delta^{202}\text{Hg}$ and $\Delta^{199}\text{Hg}$ with increasing depth of occurrence and discrete isotopic signatures of epipelagic prey ($\delta^{202}\text{Hg}$: 0.74 to 1.49‰; $\Delta^{199}\text{Hg}$: 1.76–2.96‰) and mesopelagic prey ($\delta^{202}\text{Hg}$: 0.09 to 0.90‰; $\Delta^{199}\text{Hg}$: 0.62–1.95‰) allowed the use of Hg isotopes to track PBFT foraging depth. An isotopic mixing model was used to estimate the dietary proportion of mesopelagic prey in PBFT, which ranged from 17% to 55%. Increased mesopelagic foraging was significantly correlated with slower growth and higher MeHg concentrations in PBFT. The slower observed growth rates suggest that prey availability and quality could reduce the production of PBFT biomass.



INTRODUCTION

Open ocean food webs are dynamically changing due to a combination of climate variability and fisheries exploitation.^{1–3} The relative abundance of energetically rich, epipelagic prey fluctuates with ocean temperature, climate cycles, and removal by “forage fish” fisheries.^{1,4–7} Periods of lower epipelagic prey abundance may decrease the availability of optimal prey to pelagic predators such as some tunas, billfish, and sharks, potentially leading them to exploit mesopelagic prey assemblages that tend to be more scattered, slower-growing, and of lower energetic quality.^{8,9} Such a shift requires predators to consume more prey to meet the same bioenergetic demands,

and could potentially decrease predatory fish biomass through reductions in growth rates.¹⁰ Foraging in mesopelagic regions has also been associated with increased exposures to bioaccumulative contaminants such as methylmercury (MeHg) that have higher concentrations in subsurface waters.^{11–13} Here, we explore the influence of mesopelagic feeding on Pacific bluefin tuna (*Thunnus orientalis*) growth and

Received: December 15, 2017

Revised: April 24, 2018

Accepted: May 15, 2018

Published: May 15, 2018

MeHg accumulation using information derived from Hg stable isotopes.

MeHg biomagnifies in marine food webs, reaching concentrations in top marine predators that are generally a million times greater than seawater or more.¹⁴ Large pelagic marine fishes have some of the highest MeHg concentrations in edible muscle tissue.¹⁵ MeHg concentrations in tuna vary by species, with high concentrations in large-bodied bluefin species and lowest concentrations in smaller skipjack tunas.^{15,16} Tuna species such as bluefin, yellowfin, skipjack, albacore, and bigeye contribute approximately 40% of consumed MeHg to the U.S. population.¹⁶ Lower fish growth rates have been shown to increase MeHg accumulation in marine and freshwater ecosystems^{17,18} but the relative importance of growth compared to diet composition and other factors (e.g., water temperature, trophic level) is poorly understood for marine species.^{19–21}

Naturally occurring Hg isotopes in biological tissues show promise as a new empirical source of data on fish foraging behavior and environmental sources of MeHg.^{22–26} Blum et al.²⁴ found that $\Delta^{199}\text{Hg}$ and $\delta^{202}\text{Hg}$ values in offshore pelagic marine species are effective tracers of foraging depth due to a decrease in photochemically driven Hg isotope fractionation with increasing depth. Minimal Hg isotope fractionation is thought to occur during MeHg trophic transfer from zooplankton to fish.^{27,28} This means that Hg isotopic signatures measured in fish provide information on dietary MeHg exposure sources.^{23,25,28} Here we examine the utility of Hg isotopic signatures for differentiating relative consumption of epipelagic and mesopelagic prey by individual PBFT. PBFT are an endothermic tuna species, shown to have the capacity for deep-diving behavior and a diverse diet. They are born in the western Pacific, and in their first or second year of life an unknown proportion migrate to the eastern Pacific to feed on prey resources based on local prey abundance.^{29–34} PBFT are highly migratory predators capable of foraging in a wide range of water column depths and geographic locations. Thus, they are a useful model species for testing the effects of varying foraging depth on growth rate and Hg concentrations.

The main objectives of this study are to characterize variability in feeding depths of PBFT and associated impacts on growth rates and MeHg tissue burdens. Here we present new data on Hg isotopic composition and MeHg concentrations of PBFT and their prey from various depths in the eastern and western North Pacific Ocean. We use Hg isotope composition as a proxy for feeding depths of PBFT and estimate PBFT growth rates based on otolith microstructure.³⁵ We then relate feeding depth to MeHg burdens and growth.

MATERIALS AND METHODS

Sample Collection and Processing. PBFT samples ($n = 24$) were collected from recreational angler catch off San Diego, CA as part of NOAA's biological sampling program in 2012. PBFT were collected from 4 August to 25 September 2012. PBFT in the eastern Pacific Ocean (EPO) in their first year of life or early in their second are known to be recent migrants from the western Pacific Ocean (WPO),^{29,30,32} while older PBFT can vary from >1 year residency in the EPO to recent migration from the WPO.^{29,30,32} Thus, PBFT were selected from a narrow size range, and focused on small individuals (66.3–76.0 cm FL) to minimize differences in migratory histories. Selection of these small fish, combined with information on migratory histories from otolith micro-

chemistry,³⁵ allowed for minimization of the confounding factor of varying migratory histories, especially use of the EPO versus the WPO.

PBFT ages based on sagittal otolith analysis ranged from 328 to 498 days,³⁵ with an estimated coefficient of variation of 5.7%. Individual PBFT weight could not be directly and accurately determined from samples provided by fishermen due to variable treatment of fish (blood removed, viscera removed, etc.). Muscle samples (~ 20 g) were obtained from the dorsal musculature ~ 2 cm below the skin. PBFT prey (Supporting Information (SI) Table S1) were collected directly in the field or from predator stomach contents. All prey were identified to genus or species using morphological characters. Prey from the WPO were collected from surface neuston tows, deep Ocean Research Institute (ORIs), and Isaacs-Kidd Midwater Trawls (IKMTs) during two research cruises in May and September 2013. Prey from the EPO were obtained both by trawl net in July 2015 off central CA and from stomach contents.³³ Muscle tissue was collected from the dorsal musculature below the skin (fish), from the mantle (cephalopods), or from within the carapace (crustaceans).

Hg Concentration, Prey Energy Density, and Prey Categorization. All samples were freeze-dried and homogenized using a Wig-L-Bug tissue grinder prior to any chemical analysis. The total Hg (THg) content of all PBFT and prey white muscle tissue was measured using a Nippon MA-3000 direct thermal decomposition Hg analyzer. The average recovery of the certified reference material (DORM-4) was $98.3 \pm 6.1\%$ SD ($n = 4$). Standard solution and DORM-4 calibration checks were performed every ten samples to monitor stability of the instrument. Samples were run in duplicate for every 10 samples, and overall variation of duplicates was $<3\%$. Hg concentrations are reported in $\mu\text{g g}^{-1}$ dw, and means as mean ($\mu\text{g g}^{-1}$ dw) \pm SD.

All samples with adequate mass were analyzed for MeHg. Lyophilized and powdered samples were digested in 5 N HNO_3 at 60°C overnight and neutralized with 8 M KOH. MeHg was measured using a Tekran 2700 Automated MeHg Analysis System following EPA method 1630.³⁶ Recoveries of certified reference material DORM-4 (fish muscle) and TORT-3 (lobster hepatopancreas) were $86\% \pm 6.3\%$ SD ($n = 8$). Variability among sample duplicates was $10\% \pm 4.8\%$ ($n = 9$). For prey samples with inadequate tissue mass for MeHg analyses, concentrations were estimated by using species-specific mean MeHg as a fraction of total Hg (%) from the same species. Hereafter the % of THg present as MeHg is referred to as %MeHg.

Mean energy density values (kJ g^{-1} ww) were obtained for each prey species analyzed for Hg from a literature survey of species-specific values (Figure 1; SI Table S2). When available, species- and basin-specific energy densities were chosen. For cephalopods, a mean energy density from nine pelagic cephalopods in the EPO was used.³⁷ When unavailable for WPO fish species, energy density of that species in the EPO was used. We also obtained peak abundance and depth ranges for each species from the literature (SI Table S2).

Hg Isotope analysis. Approximately 0.1–0.2 g of ground sample was digested (120°C , 6 h) in a 4 mL acid mixture ($\text{HCl}:\text{HNO}_3 = 1:3$, v:v) for Hg isotope analysis, following previous studies.^{25,38,39} Four types of certified reference materials (TORT-2, TORT-3, DORM-2, DORM-4) and blanks ($n = 5$) were prepared in the same way as tissue samples. Based on measured total Hg concentrations, the digest solutions were

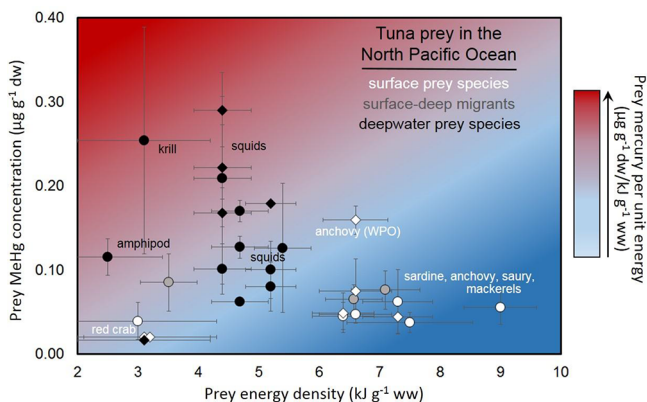


Figure 1. Energy density ($\text{kJ g}^{-1} \text{ww}$), methylmercury (MeHg) concentrations ($\mu\text{g g}^{-1} \text{dw}$), and depth distribution of pelagic prey in the eastern (circles) and western (diamonds) North Pacific Ocean. Symbols show means (error bars ± 1 SD) for surface foraging fish, diel-vertically migrating, and deepwater (mesopelagic and bathypelagic) prey. Prey energy densities are based on literature values (SI Table S2).

diluted to $0.3\text{--}1.0 \text{ ng mL}^{-1}$, depending on the availability of sample mass. A Neptune Plus multicollector inductively coupled plasma mass spectrometer (MC-ICP-MS) housed at Wisconsin State Laboratory of Hygiene was used to measure Hg isotopes. Details of instrumentation setup, operation conditions, and analytical methods are described in Yin et al.⁴⁰ and Li et al.²⁵ Total Hg in the diluted solutions was also monitored by MC-ICP-MS using ^{202}Hg signals, which yielded mean recoveries of $93 \pm 9.2\%$ and $92 \pm 11\%$ for fish samples ($n = 75$) and certified reference materials (CRMs; $n = 10$), respectively. The sensitivity for ^{202}Hg during Hg isotope analysis is estimated to be $1.0\text{--}1.2 \text{ V}$ per $\text{ng mL}^{-1} \text{ Hg}$. The signals for ^{202}Hg were $< 0.02 \text{ V}$ for acid blanks. Hg isotope values of UM-Almadén secondary Hg standard and CRMs are comparable to previous literature data^{25,41–43} (SI Table S3). Total Hg concentrations in acid digests measured by MC-ICP-MS ranged from 0.32 to 1.11 ng mL^{-1} (SI Tables S1 and S4).

Following the protocols suggested by Blum & Bergquist,⁴⁴ mass dependent fractionation (MDF) is reported using $\delta^{202}\text{Hg}$ notation in units of per mil (‰) referenced to the NIST-3133 Hg standard (eq 1). Mass independent fractionation (MIF), noted as $\Delta^{xxx}\text{Hg}$, is expressed as the difference between the measured $\delta^{xxx}\text{Hg}$ and the theoretically predicted based on MDF (eq 2).

$$\delta^{202}\text{Hg}(\text{‰}) = \left(\frac{{}^{202}\text{Hg}/{}^{198}\text{Hg}_{\text{sample}}}{{}^{202}\text{Hg}/{}^{198}\text{Hg}_{\text{NIST3133}}} \right) - 1 \quad (1)$$

$$\Delta^{xxx}\text{Hg} \approx \delta^{xxx}\text{Hg} - \delta^{202}\text{Hg} \times \beta \quad (2)$$

where β is equal to 0.252 for ^{199}Hg , 0.5024 for ^{200}Hg , 0.752 for ^{201}Hg .^[23] Ratios of $\Delta^{199}\text{Hg}/\Delta^{201}\text{Hg}$ and $\Delta^{199}\text{Hg}/\delta^{202}\text{Hg}$ were calculated using the slope from York regression, which accounts for errors in independent and dependent variables.⁴⁵

Mixing Model Estimates of PBFT Diet. A Bayesian mixing model (MixSIR)⁴⁶ was used to estimate consumption of epipelagic and mesopelagic prey by PBFT. Prey were grouped according to region collected (EPO or WPO) and vertical distribution (epipelagic or mesopelagic) as inputs to the model to assess PBFT use of vertical foraging habitat. Diel vertical migrating species were grouped with mesopelagic prey because

bluefin tunas have been shown to feed primarily during daytime,^{47,48} when these prey are in deeper waters.³³ Overall prey group means (\pm SD) for $\delta^{202}\text{Hg}$ and $\Delta^{199}\text{Hg}$ were calculated for these four groups: WPO epipelagic prey, WPO mesopelagic prey, EPO epipelagic prey, and EPO mesopelagic prey (SI Table S2). Due to the difference in slopes and Hg stable isotope values of prey in the WPO and EPO, simple grouping of mesopelagic prey and epipelagic prey was not possible (see Figure 2b) and epipelagic and mesopelagic prey

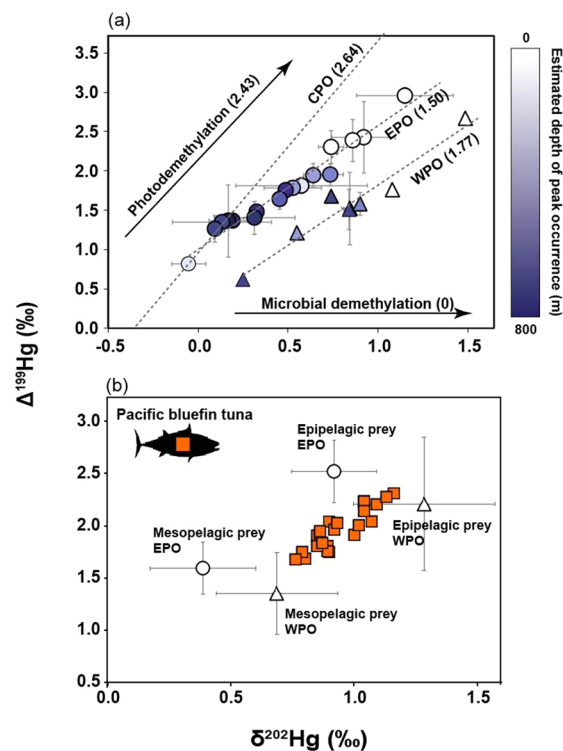


Figure 2. Hg isotope composition ($\delta^{202}\text{Hg}$ and $\Delta^{199}\text{Hg}$) of pelagic prey species in the North Pacific Ocean. (a) Measured Hg isotope values for pelagic fish in the eastern Pacific Ocean (EPO) (circles) and western Pacific Ocean (WPO) (triangles) from this study, compared to those harvested from the central Pacific Ocean (CPO) near Hawaii.²⁴ Numbers in parentheses indicate the $\Delta^{199}\text{Hg}/\delta^{202}\text{Hg}$ slope of the linear regression (dashed line) in each geographic region. Also shown is the $\Delta^{199}\text{Hg}/\delta^{202}\text{Hg}$ slope for photochemical degradation and microbial demethylation of MeHg based on experimental data simulated with 1 mg/L DOC .²³ (b) Observed Hg isotope values of Pacific bluefin tuna (orange squares) and prey items from WPO (triangles) and EPO (circles). Isotope ratios of prey groupings determined by depth: epipelagic species that spend most time in the mixed layer above the thermocline, and mesopelagic prey that spend most time at or below the thermocline (see Figure 1 for prey depth distributions).

had to be separated by region (WPO and EPO). The four overall prey group means (\pm SD) of Hg isotope values of $\delta^{202}\text{Hg}$ and $\Delta^{199}\text{Hg}$ were used as inputs for the Bayesian mixing model.

To generate mixing model diet estimates, we used uninformed priors (no assumed a priori diet information in the model) and ran 10^6 iterations. Quality assessment of diet estimates was based on model outputs of posterior draws ($>10^3$) and the ratio between “best draw” posterior and total posterior density (<0.01). Relative contributions of each prey group to PBFT diet are based on posterior distributions from

mixing model outputs and reported as medians with associated 5–95% credible intervals. Estimates of epipelagic and mesopelagic diet inputs for each PBFT were calculated by combining median estimates of epipelagic and mesopelagic diet from the WPO and EPO. These values are reported for each fish for each region (see SI Table S5) and summed mesopelagic contributions from both the WPO and EPO are used in analyses (e.g., Figure 3).

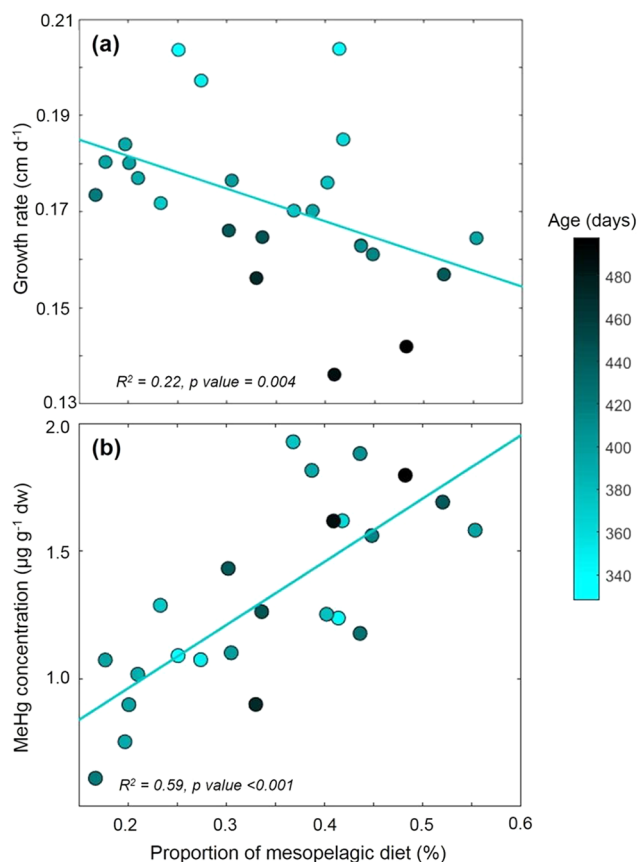


Figure 3. Correlations between mesopelagic diet proportions of Pacific bluefin tuna (*Thunnus orientalis*) derived from Hg isotope composition, PBFT growth rate (cm d^{-1}), and MeHg tissue burdens ($\mu\text{g g}^{-1} \text{dw}$). (a) Relationship between proportion of mesopelagic diet and growth rate, calculated for each PBFT based on the age and size at capture; (b) Relationship between proportion of mesopelagic diet and measured PBFT MeHg concentrations. Linear fit, R^2 and p -values shown are for linear regressions.

PBFT Growth Rates and MeHg Burdens. An instantaneous growth rate was determined for each PBFT by dividing measured length by age (days) from otolith analysis following the simple equation:

$$G(\text{cm d}^{-1}) = \text{FL}(\text{cm})/\text{age}(\text{days}) \quad (3)$$

Where G is instantaneous growth rate and FL is directly measured length (fork length) in cm, and age is from otolith microstructure estimates. This provides an instantaneous growth rate at time of capture. This was deemed appropriate by the fact that growth of PBFT at the sizes in this study have been shown to be essentially linear.^{49,50}

RESULTS

Measured MeHg concentrations and literature-reported energy contents of prey from the EPO and WPO are significantly different between epipelagic and mesopelagic zones (Figure 1). Surface-associated prey have significantly higher energy density ($6.6 \pm 2.0 \text{ SD kJ g}^{-1} \text{ ww}$) and lower MeHg concentrations ($0.05 \pm 0.01 \mu\text{g g}^{-1} \text{ dw}$), than mesopelagic prey ($4.2 \pm 0.84 \text{ kJ g}^{-1} \text{ ww}$; $0.13 \pm 0.06 \mu\text{g MeHg g}^{-1} \text{ dw}$) ($p < 0.01$, Tukey's HSD test). Species classified as primarily diel vertical migrators have intermediate MeHg concentrations ($0.08 \pm 0.01 \mu\text{g g}^{-1} \text{ dw}$) and energy density ($5.4 \pm 1.1 \text{ kJ g}^{-1} \text{ ww}$) values which are not significantly different from surface or deepwater prey ($p > 0.05$, Tukey's HSD test).

THg in PBFT ranged from 0.61 to 1.93 THg ($\mu\text{g g}^{-1} \text{ dw}$; mean $1.31 \mu\text{g g}^{-1} \text{ dw} \pm 0.37$). MeHg measurements showed that THg in PBFT was predominantly in the form of MeHg ($99\% \text{ MeHg} \pm 6\% \text{ SD}$). Prey THg ranged from 0.01 to 1.76 THg ($\mu\text{g g}^{-1} \text{ dw}$), with an overall mean of $0.13 \mu\text{g g}^{-1} \text{ dw} \pm 0.19$. Correlations between size and age of PBFT and MeHg concentrations were analyzed, and these relationships were not statistically significant.

The fraction of THg in muscle tissue as MeHg (%MeHg) in prey species was also high ($85\% \pm 18\%$), and reached 100% in several prey species (Pacific mackerel *Scomber japonicus*, market squid *Doryteuthis opalescens*, blacktip squid *Gonatus onyx*, and armhook squid *Gonatopsis borealis*). The range of %MeHg in prey fish and squid (mean $90\% \pm 9\%$; range 74%–100%) was significantly higher than in pelagic crustaceans ($57\% \pm 9\%$) (Mann–Whitney U-Test, $p = 0.0044$). Pelagic red crab (*Pleuroncodes planipes*) had the lowest %MeHg ($32\% \pm 6\%$).

In prey, both $\Delta^{199}\text{Hg}$ and $\delta^{202}\text{Hg}$ values generally decrease with increasing depth (Figure 2a, SI Figure S1). Slopes of $\Delta^{199}\text{Hg}/\delta^{202}\text{Hg}$ in muscle tissue of prey species in the EPO ($1.50 \pm 0.02 \text{ SE}$) and WPO ($1.77 \pm 0.06 \text{ SE}$) are shallower than experimentally determined slopes of photodemethylation in lab studies ($2.43 \pm 0.10 \text{ SE}$) and for muscle tissue in pelagic fish from the CPO ($2.64 \pm 0.24 \text{ SE}$)^{23,24} (Figure 2a). The highest $\Delta^{199}\text{Hg}$ and $\delta^{202}\text{Hg}$ values are found in surface foraging fish, including flying fish (*Exocoetidae* spp.) in the WPO and Pacific mackerel (*Scomber japonicus*) in the EPO (Figure 2a and SI Figure S1). The $\Delta^{199}\text{Hg}$ values of flying fish ($\sim 5\text{‰}$) observed in the central Pacific Ocean (CPO) are higher than those in surface fish in the EPO and WPO ($< 3\text{‰}$) (Figure 2a).

Hg isotope values of PBFT in this study fall between prey in the WPO and EPO (Figure 2b). Some $\delta^{202}\text{Hg}$ and $\Delta^{199}\text{Hg}$ values measured in individual PBFT overlap with surface-associated prey, and others overlap with deeper mesopelagic prey (Figure 2b). Bayesian mixing model results for Hg isotopes indicate that 28% diet is from mesopelagic prey for this PBFT data set (including both the EPO and WPO). The mesopelagic prey proportion ranges from 19% to 53% across individual PBFT (median estimates; see SI Table S5 for credible intervals). There is a statistically significant (linear regression, $P = 0.004$) decline in the growth rate of PBFT, and increase in muscle tissue MeHg burdens (linear regression, $P < 0.001$), with increasing proportion of mesopelagic prey as determined from Bayesian mixing model results (Figure 3). PBFT growth rates based on measured length and otolith-derived age varied from 0.18 to 0.25 cm d^{-1} , with a mean of $0.017 \text{ cm d}^{-1} \pm 0.02 \text{ SD}$. Proportion of mesopelagic prey in diet explains approximately 22% of the variability in PBFT

growth and 59% of the variability in PBFT muscle MeHg burdens (Figure 3).

DISCUSSION

In the WPO, epipelagic prey of juvenile PBFT > 25 cm include forage fish such as herring (*Etrumeus teres*), sardine (*Sardinops melanostictus*) and anchovy (*Engraulis japonicus*), and mesopelagic prey include lightfish (*Maurolicus japonicus*) and mesopelagic squids.^{51–53} Depending on prey availability, juvenile PBFT in the EPO feed upon epipelagic forage species including anchovy (*Engraulis mordax*), sardine (*Sardinops sagax*), and pelagic red crab (*Pleuroncodes planipes*) as well as mesopelagic fish, squids, and crustaceans.^{33,34,54}

As hypothesized, measured MeHg concentrations and energy contents of PBFT prey from the EPO and WPO are significantly different between epipelagic and mesopelagic zones, with higher energy density and lower MeHg in surface prey (Figure 1). The decrease of $\Delta^{199}\text{Hg}$ and $\delta^{202}\text{Hg}$ values with increasing depth of prey (Figure 2a, Figure S1) supports the hypothesis put forward by Blum et al.²⁴ that MeHg undergoes a greater extent of photochemical degradation in shallower waters compared to deeper waters, which is reflected in the Hg isotope composition of different predatory fish and their prey.

The highest $\Delta^{199}\text{Hg}$ and $\delta^{202}\text{Hg}$ values found in the surface foraging flying fish (*Exocoetidae* spp.) in the WPO and Pacific mackerel (*Scomber japonicus*) in the EPO (Figure 2a and SI Figure S1) indicate higher photochemical MeHg demethylation in more epipelagic, well-lit waters. The higher $\Delta^{199}\text{Hg}$ values of flying fish observed in the CPO than those in surface fish in the EPO and WPO may reflect more extensive photochemical MeHg demethylation in the CPO compared to the EPO and WPO. In the pelagic Pacific Ocean the concentrations of dissolved organic carbon (DOC) are low and relatively homogeneous compared to lakes and estuarine ecosystems.^{55,56}

Prior modeling shows that photochemical reduction dominates the redox chemistry occurring in the ocean.^{57,58} This is consistent with satellite data on primary productivity showing lower annual productivity in the CPO, allowing greater light penetration.⁵⁹

Life history information from prior work indicates that PBFT analyzed here recently migrated from WPO waters off Japan and subsequently foraged in the EPO for several months.^{29,31,32,53} This is consistent with the observed Hg isotope values of PBFT, which reflect a mix of prey consumption from both ocean basins (Figure 2b, SI Table S4). The overlap of some individual PBFT $\delta^{202}\text{Hg}$ and $\Delta^{199}\text{Hg}$ values with surface-associated prey and others with deeper mesopelagic prey suggests variable feeding depths across individuals (Figure 2b). The Bayesian mixing model-derived estimates of 19%–53% mesopelagic diet (SI Table S5) are consistent with previous and current PBFT diet studies in the WPO and EPO that used both dietary analysis and conventional chemical tracers (e.g., $\delta^{13}\text{C}$ and $\delta^{15}\text{N}$) which suggested a wide range of PBFT forage prey, but could not quantify differences between epipelagic and mesopelagic foraging.^{29,54,60} Mixing model results also allowed for comparison between epipelagic and mesopelagic feeding between ocean basins. The highest dietary inputs (41% \pm 8%) were from WPO epipelagic prey, with 21% \pm 6% from WPO mesopelagic prey (see SI Table S5). EPO meso- and epipelagic prey input values (14% \pm 4%, 25% \pm 3%) were more similar to each other, suggesting that juvenile PBFT in this particular study may have relied

more on mesopelagic prey resources in the EPO than in the WPO. Overall, our analysis illustrates the value of Hg stable isotopes as tracers in marine systems for distinguishing organism feeding depth, which more conventional chemical tracers (e.g., $\delta^{13}\text{C}$ and $\delta^{15}\text{N}$) cannot easily achieve (SI Figure S2).

Lab experiments that simulated MeHg photodegradation in freshwater settings provide estimated slopes of $\Delta^{199}\text{Hg}/\delta^{202}\text{Hg}$ that range between 2.43 and 4.79 at DOC concentrations between 1 and 10 mg L⁻¹ in freshwater solution. Blum et al.²⁴ find a very similar slope (2.64) in CPO pelagic fish and suggest that photodemethylation is the dominant process of demethylation in the central Pacific Ocean. Our observation of much shallower slopes of $\Delta^{199}\text{Hg}/\delta^{202}\text{Hg}$ in the EPO and WPO prey muscle in this study compared to CPO pelagic fish and experimental slopes suggests that photodemethylation is not exclusively responsible for the Hg isotope fractionation observed in PBFT and their prey. In lab experiments, microbial demethylation resulted in residual MeHg that had higher $\delta^{202}\text{Hg}$ values than reactant, but produced no changes of $\Delta^{199}\text{Hg}$.⁶¹ It is therefore possible that variability in the MeHg fraction degraded by microbes, rather than sunlight, across ocean regions can explain the observed differences in slopes. Specifically, we hypothesize that greater microbial demethylation occurs in bacterially active subsurface waters of the EPO and WPO compared to the CPO. This would result in higher $\delta^{202}\text{Hg}$ values in surface ocean fish and flatten the overall slope of $\Delta^{199}\text{Hg}/\delta^{202}\text{Hg}$ in EPO and WPO fish. Such a process would be consistent with recent observations and modeling showing a net loss of MeHg attributed to microbial demethylation in the WPO.⁶²

At constant $\Delta^{199}\text{Hg}$ values, an approximately 0.5‰ offset in $\delta^{202}\text{Hg}$ was apparent between WPO and EPO fish (Figure 2a). Because minimal fractionation has been observed between plankton and fish,⁶³ this suggests the Hg isotope composition of MeHg in seawater from the WPO is heavier than that from the EPO. The higher $\delta^{202}\text{Hg}$ values in the WPO, relative to the EPO, may result from methylation of inorganic Hg in contaminated source regions with heavier isotopic signatures in the WPO. Previous studies have reported higher total Hg concentrations in seawater from the WPO than EPO, due to enhanced Hg inputs from Asian countries.^{13,55} Other studies suggest greater abundance of anthropogenic Hg sources may lead to higher $\delta^{202}\text{Hg}$ values compared to less impacted regions.⁶⁴

PBFT growth rates, based on measured length and otolith-derived age, varied from 79% to 119% of the mean growth rate of all individuals. MeHg concentrations varied from 46% to 146% of the observed PBFT mean. The extent of mesopelagic foraging explains a substantial amount of this variability in growth (22%) and MeHg (59%). Geographic variability in foraging conditions and fluctuations in epipelagic prey abundance may cause individual PBFT to subsidize their diet with mesopelagic prey;³³ our results suggest these differences are sufficient to drive appreciable differences in PBFT growth (Figure 3b) and consequently, reduced size at age. Variability in growth rates has been reported in extensive age-growth studies of wild tunas, including PBFT,⁶⁵ which has been a source of uncertainty in stock assessments. Physiological and ecological mechanisms explaining this observed variability have not been conclusively demonstrated, likely due to challenges associated with tracking fish growth and feeding behavior in wild conditions. Electronic tagging studies provide evidence for

variability in migratory patterns and diving behavior of PBFT.^{31,33,48,53,66–70} Variability in water column use likely corresponds to individual differences in relative consumption of epipelagic and mesopelagic prey.^{31,53} Interindividual variability in foraging success linked to geographic location and environmental conditions⁴⁸ supports the interpretation of different PBFT Hg isotopic values as indicators of individual variability in prior foraging behavior.

Our results show that individual variability in foraging depth will influence growth rates of PBFT. Variable feeding in tuna, reflective of local prey abundance, is supported by previous diet studies of tuna species in the EPO. During a period of high anchovy abundance, both Pacific bluefin tuna and albacore tunas fed extensively on anchovy, but albacore diet was more diverse with anchovy being less important overall.^{33,71} During a time period of sardine and anchovy scarcity in the EPO, yellowfin, albacore, and Pacific bluefin tunas differed in vertical habitat use, diet composition, and daily energy intake.³³ Our synthesis of prey energy density data show that in the WPO and EPO regions considered, epipelagic prey is generally higher in energy, but other factors should be considered in the interpretation of our results for PBFT. For example, the mesopelagic zone can contain a high abundance of lanternfish or myctophids (rich in fatty acids) and squid, which demonstrably support several mesopelagic predator species (e.g., opah *Lampris guttatus*, swordfish *Xiphias gladius*, blue shark *Prionace glauca*, lancetfish *Alepisaurus* spp., escolar *Lepidocybium flavobrunneum*, oilfish *Ruvettus pretiosus*, and at times bigeye tuna *Thunnus obesus*^{72–75}). The success and proliferation of these predominantly mesopelagic predator species and others species (including large-bodied marine mammals^{76–79}) suggest that mesopelagic prey, and their potentially extremely high biomass in the open ocean,^{80,81} can adequately support large pelagic predators. Certain pelagic species that forage less on mesopelagic resources may be limited by physiological constraints, reliance on visual predation, or other limitations.⁸² Regardless, certain studies above and our results demonstrate that diet and feeding performance may be influenced by the availability of optimal epipelagic prey.

Certain limitations and caveats apply to analyses and conclusions presented here. Sample size of PBFT available for otolith microstructure analysis and Hg isotope analysis was limited to 24 individual PBFT, from a single year, and larger sample sizes will allow more robust conclusions. This study only included young PBFT, and it is unknown how foraging depth and resultant growth and MeHg will vary in larger, older individuals. We were only able to use instantaneous growth as our growth metric, and changes in growth with age could potentially be investigated in future captive experiments. Prey energy density changes over time, and temporal effects could also be further examined. This study intentionally addresses only feeding depth as a variable affecting growth and Hg accumulation, which can contribute to larger meta-analyses of the many factors affecting Hg levels in tuna by allowing more informed inclusion of this variable and its effects. Finally, as with most stable isotope Bayesian mixing model approaches, credibility intervals were large and median values of mesopelagic feeding should be interpreted in this context. However, despite limited sample size and the confounding variables above, we found that PBFT feeding depth significantly affects growth rate and Hg levels by applying a new tool with great promise for future, more extensive studies.

This preliminary evidence that differences in mesopelagic foraging by PBFT can lead to variability in growth rates may help to explain previously observed large interindividual differences in bluefin tuna MeHg accumulation⁸³ and growth rates.⁶⁵ Results show that ecological factors in the pelagic environment will influence MeHg concentration in tuna and other fish in the future. The lowest and highest observed PBFT growth rates measured in this study correspond to the highest and lowest extent of mesopelagic feeding. Bounds for impacts of variable mesopelagic foraging based on estimated growth rates results in length differences of ~10 cm in the oldest PBFT sampled here, corresponding to differences in mass of –30% to +40% based on PBFT length-weight relationships.⁶⁵ PBFT harvests in the EPO from 1952 to 2014 ranged from approximately 5000 to 40 000 t annually.⁸⁴ Thus, population-wide decreases in growth rate, to the lowest growth rates we observed, would result in an estimated hundreds to thousands of tons of PBFT biomass lost to decreased growth due to changes in foraging depth. This lost biomass, based on ecological shifts, could decrease the actual commercial harvest of PBFT.

Ref 84.

■ ASSOCIATED CONTENT

📄 Supporting Information

The Supporting Information is available free of charge on the ACS Publications website at DOI: 10.1021/acs.est.7b06429.

Additional information as noted in the text (PDF)

■ AUTHOR INFORMATION

Corresponding Author

*Phone: +1 (516) 680-6470; e-mail: daniel.madigan@stonybrook.edu.

ORCID

Daniel J. Madigan: 0000-0002-5718-562X

Miling Li: 0000-0001-8574-2625

David P. Krabbenhoft: 0000-0003-1964-5020

Elsie M. Sunderland: 0000-0003-0386-9548

Present Address

¶(D.J.M.) Gulf of California International Research Center, Santa Rosalía, BCS, Mexico.

Author Contributions

∞D.J.M. and M.L. contributed equally to this work.

Notes

The authors declare no competing financial interest.

■ ACKNOWLEDGMENTS

We thank the recreational anglers in San Diego who donated their catch to this study. Jun Nishikawa facilitated sample collection during research cruises off the coast of Japan. NOAA staff and volunteers assisted with sample collections, and J. Ewald assisted with sample preparation. We acknowledge financial support for this work from the USGS Toxics Hydrology Program. D.J.M. was supported by the John & Elaine French Harvard University Center for the Environment Fellowship. N.F. was supported by OCE1634024. The views expressed in this paper are solely those of the authors and the content of the paper does not represent the views or position of the U.S. Geological Survey. Any use of trade, product, or firm names in this publication is for descriptive purposes only and does not imply endorsement by the U.S. Government.

REFERENCES

- (1) Chavez, F. P.; Ryan, J.; Lluch-Cota, S. E.; Ñiquen, C. M. From anchovies to sardines and back: multidecadal change in the Pacific Ocean. *Science* **2003**, *299* (5604), 217–221.
- (2) Olson, R. J.; Popp, B. N.; Graham, B. S.; López-Ibarra, G. A.; Galván-Magaña, F.; Lennert-Cody, C. E.; Bocanegra-Castillo, N.; Wallsgrove, N. J.; Gier, E.; Alatorre-Ramírez, V.; Ballance, L. T.; Fry, B. Food-web inferences of stable isotope spatial patterns in copepods and yellowfin tuna in the pelagic eastern Pacific Ocean. *Prog. Oceanogr.* **2010**, *86* (1–2), 124–138.
- (3) Worm, B.; Barbier, E. B.; Beaumont, N.; Duffy, J. E.; Folke, C.; Halpern, B. S.; Jackson, J. B.; Lotze, H. K.; Micheli, F.; Palumbi, S. R. Impacts of biodiversity loss on ocean ecosystem services. *Science* **2006**, *314* (5800), 787–790.
- (4) Cury, P. M.; Boyd, I. L.; Bonhommeau, S.; Anker-Nilssen, T.; Crawford, R. J. M.; Furness, R. W.; Mills, J. A.; Murphy, E. J.; Österblom, H.; Paleczny, M.; Piatt, J. F.; Roux, J.-P.; Shannon, L.; Sydeman, W. J. Global seabird response to forage fish depletion - one-third for the birds. *Science* **2011**, *334* (6063), 1703–1706.
- (5) Fréon, P.; Cury, P.; Shannon, L.; Roy, C. Sustainable Exploitation of small pelagic fish stocks challenged by environmental and ecosystem changes: A review. *Bull. Mar. Sci.* **2005**, *76* (2), 385–462.
- (6) Pinsky, M. L.; Jensen, O. P.; Ricard, D.; Palumbi, S. R. Unexpected patterns of fisheries collapse in the world's oceans. *Proc. Natl. Acad. Sci. U. S. A.* **2011**, *108* (20), 8317–8322.
- (7) Essington, T. E.; Moriarty, P. E.; Froehlich, H. E.; Hodgson, E. E.; Koehn, L. E.; Oken, K. L.; Siple, M. C.; Stawitz, C. C. Fishing amplifies forage fish population collapses. *Proc. Natl. Acad. Sci. U. S. A.* **2015**, *112* (21), 6648–6652.
- (8) Vollenweider, J. J.; Heintz, R. A.; Schaufler, L.; Bradshaw, R. Seasonal cycles in whole-body proximate composition and energy content of forage fish vary with water depth. *Mar. Biol.* **2011**, *158* (2), 413–427.
- (9) Spitz, J.; Mourocq, E.; Leauté, J.-P.; Quéro, J.-C.; Ridoux, V. Prey selection by the common dolphin: Fulfilling high energy requirements with high quality food. *J. Exp. Mar. Biol. Ecol.* **2010**, *390* (2), 73–77.
- (10) Coll, M.; Libralato, S.; Tudela, S.; Palomera, I.; Pranovi, F. Ecosystem Overfishing in the Ocean. *PLoS One* **2008**, *3* (12), e3881.
- (11) Choy, C. A.; Popp, B. N.; Kaneko, J. J.; Drazen, J. C. The influence of depth on mercury levels in pelagic fishes and their prey. *Proc. Natl. Acad. Sci. U. S. A.* **2009**, *106* (33), 13865–13869.
- (12) Monteiro, L. R.; Furness, R. W. Accelerated increase in mercury contamination in North Atlantic mesopelagic food chains as indicated by time series of seabird feathers. *Environ. Toxicol. Chem.* **1997**, *16* (12), 2489–2493.
- (13) Sunderland, E. M.; Krabbenhoft, D. P.; Moreau, J. W.; Strode, S. A.; Landing, W. M. Mercury sources, distribution, and bioavailability in the North Pacific Ocean: Insights from data and models. *Global Biogeochem. Cycles* **2009**, *23* (2), n/a.
- (14) Lavoie, R. A.; Jardine, T. D.; Chumchal, M. M.; Kidd, K. A.; Campbell, L. M. Biomagnification of Mercury in Aquatic Food Webs: A Worldwide Meta-Analysis. *Environ. Sci. Technol.* **2013**, *47* (23), 13385–13394.
- (15) Karimi, R.; Fitzgerald, T. P.; Fisher, N. S. A quantitative synthesis of mercury in commercial seafood and implications for exposure in the United States. *Environ. Health Perspect.* **2012**, *120* (11), 1512–9.
- (16) Sunderland, E. M. Mercury Exposure from Domestic and Imported Estuarine and Marine Fish in the U.S. Seafood Market. *Environ. Health Perspect.* **2007**, *115* (2), 235–242.
- (17) Doyon, J.-F.; Schetagne, R.; Verdon, R. Different mercury bioaccumulation rates between sympatric populations of dwarf and normal lake whitefish (*Coregonus clupeaformis*) in the La Grande complex watershed, James Bay, Québec. *Biogeochemistry* **1998**, *40* (2–3), 203–216.
- (18) Baumann, Z.; Mason, R. P.; Conover, D. O.; Balcom, P.; Chen, C. Y.; Buckman, K. L.; Fisher, N. S.; Baumann, H. Mercury bioaccumulation increases with latitude in a coastal marine fish (Atlantic silverside, *Menidia menidia*). *Can. J. Fish. Aquat. Sci.* **2016**, *74* (7), 1009–1015.
- (19) Stafford, C. P.; Haines, T. A. Mercury contamination and growth rate in two piscivore populations. *Environ. Toxicol. Chem.* **2001**, *20* (9), 2099–2101.
- (20) Chen, C. Y.; Dionne, M.; Mayes, B. M.; Ward, D. M.; Sturup, S.; Jackson, B. P. Mercury Bioavailability and Bioaccumulation in Estuarine Food Webs in the Gulf of Maine. *Environ. Sci. Technol.* **2009**, *43* (6), 1804–1810.
- (21) Cossa, D.; Harmelin-Vivien, M.; Mellon-Duval, C.; Loizeau, V.; Averty, B.; Crochet, S.; Chou, L.; Cadiou, J. F. Influences of Bioavailability, Trophic Position, and Growth on Methylmercury in Hakes (*Merluccius merluccius*) from Northwestern Mediterranean and Northeastern Atlantic. *Environ. Sci. Technol.* **2012**, *46* (9), 4885–4893.
- (22) Blum, J. D. Applications of stable mercury isotopes to biogeochemistry. In *Handbook of Environmental Isotope Geochemistry*; Springer: Berlin, 2012; pp 229–245.
- (23) Bergquist, B. A.; Blum, J. D. Mass-dependent and -independent fractionation of Hg isotopes by photoreduction in aquatic systems. *Science* **2007**, *318* (5849), 417–420.
- (24) Blum, J. D.; Popp, B. N.; Drazen, J. C.; Choy, C. A.; Johnson, M. W. Methylmercury production below the mixed layer in the North Pacific Ocean. *Nat. Geosci.* **2013**, *6* (6), 879–884.
- (25) Li, M.; Schartup, A. T.; Valberg, A. P.; Ewald, J. D.; Krabbenhoft, D. P.; Yin, R.; Balcom, P. H.; Sunderland, E. M. Environmental origins of methylmercury accumulated in subarctic estuarine fish indicated by mercury stable isotopes. *Environ. Sci. Technol.* **2016**, *50* (50), 11559–11568.
- (26) Senn, D. B.; Chesney, E. J.; Blum, J. D.; Bank, M. S.; Maage, A.; Shine, J. P. Stable isotope (N, C, Hg) study of methylmercury sources and trophic transfer in the Northern Gulf of Mexico. *Environ. Sci. Technol.* **2010**, *44* (5), 1630–1637.
- (27) Kwon, S. Y.; Blum, J. D.; Madigan, D. J.; Block, B. A.; Popp, B. N. Quantifying mercury isotope dynamics in captive Pacific bluefin tuna (*Thunnus orientalis*). *Elementa: Science of the Anthropocene* **2016**.4000088
- (28) Kwon, S. Y.; Blum, J. D.; Carvan, M. J.; Basu, N.; Head, J. A.; Madenjian, C. P.; David, S. R. Absence of fractionation of mercury isotopes during trophic transfer of methylmercury to freshwater fish in captivity. *Environ. Sci. Technol.* **2012**, *46* (14), 7527–7534.
- (29) Madigan, D. J.; Baumann, Z.; Carlisle, A. B.; Snodgrass, O.; Dewar, H.; Fisher, N. S. Isotopic insights into migration patterns of Pacific bluefin tuna in the eastern Pacific Ocean. *Can. J. Fish. Aquat. Sci.* **2017**, *75*, 260.
- (30) Bayliff, W. H. A review of the biology and fisheries for northern bluefin tuna, *Thunnus thynnus*, in the Pacific Ocean. *FAO Fish. Technol. Pap.* **1994**, *336*, 244–295.
- (31) Boustany, A. M.; Matteson, R.; Castleton, M.; Farwell, C.; Block, B. A. Movements of Pacific bluefin tuna (*Thunnus orientalis*) in the Eastern North Pacific revealed with archival tags. *Prog. Oceanogr.* **2010**, *86* (1–2), 94–104.
- (32) Fujioka, K.; Fukuda, H.; Tei, Y.; Okamoto, S.; Kiyofuji, H.; Furukawa, S.; Takagi, J.; Estess, E.; Farwell, C. J.; Fuller, D. W.; Suzuki, N.; Ohshimo, S.; Kitagawa, T. Spatial and temporal variability in the trans-Pacific migration of Pacific bluefin tuna (*Thunnus orientalis*) revealed by archival tags. *Prog. Oceanogr.* **2018**, *162*, 52–65.
- (33) Madigan, D. J.; Carlisle, A. B.; Gardner, L. D.; Jayasundara, N.; Micheli, F.; Schaefer, K. M.; Fuller, D. W.; Block, B. A. Assessing niche width of endothermic fish from genes to ecosystem. *Proc. Natl. Acad. Sci. U. S. A.* **2015**, *112* (27), 8350–8355.
- (34) Pinkas, L. Bluefin tuna food habits. *Fish. Bull. Cal. Dept. Fish Game* **1971**, *152*, 47–63.
- (35) Baumann, H.; Wells, R. J. D.; Rooper, J. R.; Zhang, S.; Baumann, Z.; Madigan, D. J.; Dewar, H.; Snodgrass, O. E.; Fisher, N. S. Combining otolith microstructure and trace elemental analyses to infer the arrival of juvenile Pacific bluefin tuna in the California current ecosystem. *ICES J. Mar. Sci.* **2015**, *72* (7), 2128–2138.

- (36) Method 1630: Methylmercury in Water by Distillation, Aqueous Ethylation, Purge and Trap, And Cold Vapor Atomic Fluorescence Spectrometry; USEPA: Washington, DC, 1998.
- (37) Glaser, S. Interdecadal variability in predator-prey interactions of juvenile North Pacific albacore in the California Current System. *Mar. Ecol. Prog. Ser.* **2010**, *414*, 209–221.
- (38) Perrot, V.; Epov, V. N.; Pastukhov, M. V.; Grebenshchikova, V. I.; Zouiten, C.; Sonke, J. E.; Husted, S.; Donard, O. F. X.; Amouroux, D. Tracing Sources and Bioaccumulation of Mercury in Fish of Lake Baikal—Angara River Using Hg Isotopic Composition. *Environ. Sci. Technol.* **2010**, *44* (21), 8030–8037.
- (39) Perrot, V.; Pastukhov, M. V.; Epov, V. N.; Husted, S.; Donard, O. F.; Amouroux, D. Higher Mass-Independent Isotope Fractionation of Methylmercury in the Pelagic Food Web of Lake Baikal (Russia). *Environ. Sci. Technol.* **2012**, *46* (11), 5902–5911.
- (40) Yin, R.; Krabbenhoft, D. P.; Bergquist, B. A.; Zheng, W.; Lepak, R. F.; Hurley, J. P. Effects of mercury and thallium concentrations on high precision determination of mercury isotopic composition by Neptune Plus multiple collector inductively coupled plasma mass spectrometry. *J. Anal. At. Spectrom.* **2016**, *31* (10), 2060–2068.
- (41) Sherman, L.; Blum, J. Mercury stable isotopes in sediments and largemouth bass from Florida lakes, USA. *Sci. Total Environ.* **2013**, *448*, 163–175.
- (42) Tsui, M. T. K.; Blum, J. D.; Kwon, S. Y.; Finlay, J. C.; Balogh, S. J.; Nollet, Y. H. Sources and Transfers of Methylmercury in Adjacent River and Forest Food Webs. *Environ. Sci. Technol.* **2012**, *46* (20), 10957–10964.
- (43) Lepak, R. F.; Yin, R.; Krabbenhoft, D. P.; Ogorek, J. M.; DeWild, J. F.; Holsen, T. M.; Hurley, J. P. Use of stable isotope signatures to determine mercury sources in the Great Lakes. *Environ. Sci. Technol. Lett.* **2015**, *2* (12), 335–341.
- (44) Blum, J. D.; Bergquist, B. A. Reporting of variations in the natural isotopic composition of mercury. *Anal. Bioanal. Chem.* **2007**, *388* (2), 353–359.
- (45) York, D. Least squares fitting of a straight line with correlated errors. *Earth Planet. Sci. Lett.* **1968**, *5*, 320–324.
- (46) Moore, J. W.; Semmens, B. X. Incorporating uncertainty and prior information into stable isotope mixing models. *Ecol. Lett.* **2008**, *11* (5), 470–480.
- (47) Bestley, S.; Patterson, T. A.; Hindell, M. A.; Gunn, J. S. Feeding ecology of wild migratory tunas revealed by archival tag records of visceral warming. *J. Anim. Ecol.* **2008**, *77* (6), 1223–1233.
- (48) Whitlock, R. E.; Hazen, E. L.; Walli, A.; Farwell, C.; Bograd, S. J.; Foley, D. G.; Castleton, M.; Block, B. A. Direct quantification of energy intake in an apex marine predator suggests physiology drives seasonal migrations. *Sci. Adv.* **2015**, *1* (8), e1400270.
- (49) Farwell, C., Tunas in captivity. In *Tuna: Physiology, Ecology, and Evolution*; Block, B. A., Stevens, E. D., Eds., 2001; Vol. 19, pp 391–412.
- (50) Bayliff, W. H.; Ishizuka, Y.; Deriso, R. Growth, movement, and attrition of northern bluefin tuna, *Thunnus thynnus*, in the Pacific Ocean, as determined by tagging. *Inter-Am. Trop. Tuna Comm. Bull.* **1991**, *20*, 3–94.
- (51) Shimose, T.; Watanabe, H.; Tanabe, T.; Kubodera, T. Ontogenetic diet shift of age-0 year Pacific bluefin tuna *Thunnus orientalis*. *J. Fish Biol.* **2013**, *82* (1), 263–276.
- (52) Yamanaka, H. Synopsis of biological data on kuromaguro *Thunnus orientalis* (Temminck & Schlegel) 1942 (Pacific Ocean). *FAO Fish. Rep.* **1963**, *6*, 180–217.
- (53) Kitagawa, T.; Kimura, S.; Nakata, H.; Yamada, H. Why do young Pacific bluefin tuna repeatedly dive to depths through the thermocline? *Fish. Sci.* **2007**, *73* (1), 98–106.
- (54) Snodgrass, O.; Dewar, H.; Wells, D.; Thompson, A.; Kohin, S. Foraging Ecology of Tunas in the Southern California Bight (2007–2016). In *The International Tuna Conference on Tunas and Billfish*, May 15–18; Lake Arrowhead, California, 2017.
- (55) Zhang, Y.; Jacob, D. J.; Dutkiewicz, S.; Amos, H. M.; Long, M. S.; Sunderland, E. M. Biogeochemical drivers of the fate of riverine mercury discharged to the global and Arctic oceans. *Global Biogeochemical Cycles* **2015**, *29* (6), 854–864.
- (56) Schartup, A. T.; Qureshi, A.; Dassuncao, C.; Thackray, C. P.; Harding, G.; Sunderland, E. M. A Model for Methylmercury Uptake and Trophic Transfer by Marine Plankton. *Environ. Sci. Technol.* **2018**, *52* (2), 654–662.
- (57) Soerensen, A. L.; Sunderland, E. M.; Holmes, C. D.; Jacob, D. J.; Yantosca, R. M.; Skov, H.; Christensen, J. H.; Strode, S. A.; Mason, R. P. An Improved Global Model for Air-Sea Exchange of Mercury: High Concentrations over the North Atlantic. *Environ. Sci. Technol.* **2010**, *44* (22), 8574–8580.
- (58) Soerensen, A. L.; Mason, R. P.; Balcom, P. H.; Jacob, D. J.; Zhang, Y.; Kuss, J.; Sunderland, E. M. Elemental mercury concentrations and fluxes in the tropical atmosphere and ocean. *Environ. Sci. Technol.* **2014**, *48* (19), 11312–11319.
- (59) NEO NASA Earth Observations https://neo.sci.gsfc.nasa.gov/view.php?datasetId=MY1DMM_CHLORA (accessed December 15, 2016).
- (60) Shimose, T.; Watanabe, H.; Tanabe, T.; Kubodera, T. Ontogenetic diet shift of age-0 year Pacific bluefin tuna. *J. Fish Biol.* **2013**, *82*, 263.
- (61) Kritee, K.; Barkay, T.; Blum, J. D. Mass dependent stable isotope fractionation of mercury during mer mediated microbial degradation of monomethylmercury. *Geochim. Cosmochim. Acta* **2009**, *73* (5), 1285–1296.
- (62) Kim, H.; Soerensen, A. L.; Hur, J.; Heimbürger, L.-E.; Hahm, D.; Rhee, T. S.; Noh, S.; Han, S., Methylmercury mass budgets and distribution characteristics in the Western Pacific Ocean. *Environ. Sci. Technol.* **2016**, 511186.
- (63) Kwon, S. Y.; Blum, J. D.; Carvan, M. J.; Basu, N.; Head, J. A.; Madenjian, C. P.; David, S. R. Absence of fractionation of mercury isotopes during trophic transfer of methylmercury to freshwater fish in captivity. *Environ. Sci. Technol.* **2012**, *46* (14), 7527–7534.
- (64) Lepak, R. F.; Yin, R.; Krabbenhoft, D. P.; Ogorek, J. M.; DeWild, J. F.; Holsen, T. M.; Hurley, J. P. Use of stable isotope signatures to determine mercury sources in the Great Lakes. *Environ. Sci. Technol. Lett.* **2015**, *2*, 335–341.
- (65) Shimose, T.; Tanabe, T.; Chen, K.-S.; Hsu, C.-C. Age determination and growth of Pacific bluefin tuna, *Thunnus orientalis*, off Japan and Taiwan. *Fish. Res.* **2009**, *100* (2), 134–139.
- (66) Kitagawa, T.; Kimura, S.; Nakata, H.; Yamada, H.; Nitta, A.; Sasai, Y.; Sasaki, H. Immature Pacific bluefin tuna, *Thunnus orientalis*, utilizes cold waters in the Subarctic Frontal Zone for trans-Pacific migration. *Environ. Biol. Fishes* **2009**, *84* (2), 193–196.
- (67) Kitagawa, T.; Boustany, A. M.; Farwell, C. J.; Williams, T. D.; Castleton, M. R.; Block, B. A. Horizontal and vertical movements of juvenile bluefin tuna (*Thunnus orientalis*) in relation to seasons and oceanographic conditions in the eastern Pacific Ocean. *Fish. Oceanogr.* **2007**, *16* (5), 409–421.
- (68) Kitagawa, T.; Kimura, S.; Nakata, H.; Yamada, H. Diving behavior of immature, feeding Pacific bluefin tuna (*Thunnus thynnus orientalis*) in relation to season and area: the East China Sea and the Kuroshio-Oyashio transition region. *Fish. Oceanogr.* **2004**, *13* (3), 161–180.
- (69) Itoh, T.; Tsuji, S.; Nitta, A. Migration patterns of young Pacific bluefin tuna (*Thunnus orientalis*) determined with archival tags. *Fish. Bull.* **2003**, *101* (3), 514–535.
- (70) Itoh, T.; Tsuji, S.; Nitta, A. Swimming depth, ambient water temperature preference, and feeding frequency of young Pacific bluefin tuna (*Thunnus orientalis*) determined with archival tags. *Fish. Bull.* **2003**, *101*, 535–544.
- (71) Pinkas, L.; Oliphant, M. S.; Iverson, I. L. K. Food habits of albacore, bluefin tuna, and bonito in California waters. *Fish. Bull. Cal. Dept. Fish Game* **1971**, *152*, 1–105.
- (72) Choy, C. A.; Wabnitz, C. C. C.; Weijerman, M.; Woodworth-Jefcoats, P. A.; Polovina, J. J. Finding the way to the top: how the composition of oceanic mid-trophic micronekton groups determines apex predator biomass in the central North Pacific. *Mar. Ecol. Prog. Ser.* **2016**, *549*, 9–25.

(73) Choy, C. A.; Popp, B. N.; Hannides, C. C. S.; Drazen, J. C. Trophic structure and food resources of epipelagic and mesopelagic fishes in the North Pacific Subtropical Gyre ecosystem inferred from nitrogen isotopic compositions. *Limnol. Oceanogr.* **2015**, *60* (4), 1156–1171.

(74) Potier, M.; Marsac, F.; Cherel, Y.; Lucas, V.; Sabatié, R.; Maury, O.; Ménard, F. Forage fauna in the diet of three large pelagic fishes (lancetfish, swordfish and yellowfin tuna) in the western equatorial Indian Ocean. *Fish. Res.* **2007**, *83* (1), 60–72.

(75) Preti, A.; Soykan, C.; Dewar, H.; Wells, R.; Spear, N.; Kohin, S. Comparative feeding ecology of shortfin mako, blue and thresher sharks in the California Current. *Environ. Biol. Fishes* **2012**, *95*, 1–20.

(76) Robinson, P. W.; Costa, D. P.; Crocker, D. E.; Gallo-Reynoso, J. P.; Champagne, C. D.; Fowler, M. A.; Goetsch, C.; Goetz, K. T.; Hassrick, J. L.; Hückstädt, L. A.; Kuhn, C. E.; Maresh, J. L.; Maxwell, S. M.; McDonald, B. I.; Peterson, S. H.; Simmons, S. E.; Teutschel, N. M.; Villegas-Amtmann, S.; Yoda, K. Foraging Behavior and Success of a Mesopelagic Predator in the Northeast Pacific Ocean: Insights from a Data-Rich Species, the Northern Elephant Seal. *PLoS One* **2012**, *7* (5), e36728.

(77) Peterson, S. H.; Ackerman, J. T.; Costa, D. P., Marine foraging ecology influences mercury bioaccumulation in deep-diving northern elephant seals. *Proc. R. Soc. London, Ser. B* **2015**, *282* (1810), 20150710

(78) Kawakami, T. A review of sperm whale food. *Sci. Rep. Whales Res. Inst* **1980**, *32*, 199–218.

(79) Smith, S. C.; Whitehead, H. The diet of Galapagos sperm whales *Physeter macrocephalus* as indicated by fecal sample analysis. *Mar. Mammal Sci.* **2000**, *16* (2), 315–325.

(80) Irigoien, X.; Klevjer, T. A.; Røstad, A.; Martinez, U.; Boyra, G.; Acuña, J. L.; Bode, A.; Echevarria, F.; Gonzalez-Gordillo, J. I.; Hernandez-Leon, S.; Agusti, S.; Aksnes, D. L.; Duarte, C. M.; Kaartvedt, S., Large mesopelagic fishes biomass and trophic efficiency in the open ocean. *Nat. Commun.* **2014**, *5*. DOI: [10.1038/ncomms4271](https://doi.org/10.1038/ncomms4271)

(81) Gjøsæter, J.; Kawaguchi, K. *A Review of the World Resources of Mesopelagic Fish*; Food & Agriculture Organization, 1980.

(82) Block, B. A.; Jonsen, I. D.; Jorgensen, S. J.; Winship, A. J.; Shaffer, S. A.; Bograd, S. J.; Hazen, E. L.; Foley, D. G.; Breed, G. A.; Harrison, A. L.; Ganong, J. E.; Swithenbank, A.; Castleton, M.; Dewar, H.; Mate, B. R.; Shillinger, G. L.; Schaefer, K. M.; Benson, S. R.; Weise, M. J.; Henry, R. W.; Costa, D. P. Tracking apex marine predator movements in a dynamic ocean. *Nature* **2011**, *475*, 86–90.

(83) Lee, C. S.; Lutcavage, M. E.; Chandler, E.; Madigan, D. J.; Cerrato, R. M.; Fisher, N. S. Declining mercury concentrations in bluefin tuna reflect reduced emissions to the North Atlantic Ocean. *Environ. Sci. Technol.* **2016**, *50* (23), 12825–12830.

(84) ISC Pacific Bluefin Stock Assessment. *International Scientific Committee for Tuna and Tuna-like Species in the North Pacific Ocean*; La Jolla, CA, 2016.